ARTICLE

BIOTECHNOLOGY and BIOENGINEERING

Improving Fold Activation of Small Transcription Activating RNAs (STARs) with Rational RNA Engineering Strategies

Sarai Meyer, James Chappell, Sitara Sankar, Rebecca Chew, Julius B. Lucks

School of Chemical and Biomolecular Engineering, Cornell University, Ithaca, New York 14853; telephone: 607-255-3601; fax: 1-607-255-9166; e-mail: jblucks@cornell.edu

ABSTRACT: Regulatory RNAs have become integral components of the synthetic biology and bioengineering toolbox for controlling gene expression. We recently expanded this toolbox by creating small transcription activating RNAs (STARs) that act by disrupting the formation of a target transcriptional terminator hairpin placed upstream of a gene. While STARs are a promising addition to the repertoire of RNA regulators, much work remains to be done to optimize the fold activation of these systems. Here we apply rational RNA engineering strategies to improve the fold activation of two STAR regulators. We demonstrate that a combination of promoter strength tuning and multiple RNA engineering strategies can improve fold activation from 5.4-fold to 13.4-fold for a STAR regulator derived from the pbuE riboswitch terminator. We then validate the generality of our approach and show that these same strategies improve fold activation from 2.1-fold to 14.6-fold for an unrelated STAR regulator, opening the door to creating a range of additional STARs to use in a broad array of biotechnologies. We also establish that the optimizations preserve the orthogonality of these STARs between themselves and a set of RNA transcriptional repressors, enabling these optimized STARs to be used in sophisticated circuits.

Biotechnol. Bioeng. 2016;113: 216–225.

KEYWORDS: synthetic biology; RNA engineering; transcriptional activation; transcriptional regulator; small transcription activating RNA (STAR)

The authors declare competing financial interest. The authors have submitted a provisional patent application (No. 61/981,241) for the technologically important developments included in this article.

Correspondence to: J. B. Lucks

Contract grant sponsor: National Science Foundation Graduate Research Fellowship Program

Contract grant number: DGE-1144153

Contract grant sponsor: Defense Advanced Research Projects Agency Young Faculty Award

Contract grant number: N66001-12-1-4254

Contract grant sponsor: Office of Naval Research Young Investigators Program Award

Contract grant number: N00014-13-1-0531

Contract grant sponsor: NSF CAREER Award

Contract grant number: 1452441

Contract grant sponsor: Cornell University College of Engineering's 'Engineering Learning Initiatives' Undergraduate Research Grant Program

Received 20 February 2015; Revision received 4 June 2015; Accepted 23 June 2015

Accepted manuscript online 1 July 2015;

Article first published online 9 September 2015 in Wiley Online Library (http://onlinelibrary.wiley.com/doi/10.1002/bit.25693/abstract).

DOI 10.1002/bit.25693

Introduction

Natural and engineered RNA regulators have become powerful components of our toolbox for precisely regulating gene expression (Chappell et al., 2013). This is in large part due to advances in our understanding of RNA biology that have uncovered a vast range of regulatory functions performed by naturally occurring RNAs (Cech and Steitz, 2014; Chappell et al., 2013). Many of these functions involve the regulation of the fundamental processes of gene expression, including mRNA degradation (Collins et al., 2007; Filipowicz et al., 2008; Storz et al., 2011), translation (Gottesman and Storz, 2011; Nou and Kadner, 2000; Winkler et al., 2002), and transcription elongation (Brantl and Wagner, 2000). Recent work has further revealed how these functions are intimately linked to the structure of the regulatory RNAs and the structural rearrangements they induce in their targets (DebRoy et al., 2014). This in turn has enabled significant advances in design approaches that use computational RNA structure prediction algorithms to design synthetic RNAs that adopt specific conformations to perform their regulatory function (Green et al., 2014; Rodrigo et al., 2012). RNA regulators thus represent a versatile and designable platform for controlling gene expression and have been used in a number of recent applications, including the creation of synthetic RNA regulatory gene expression switches (Ceres et al., 2013a; Kennedy et al., 2014; Lynch et al., 2007; Wachsmuth et al., 2013), RNA—only logic gates and circuits (Chappell et al., 2015; Lucks et al., 2011; Xie et al., 2011), RNA transcriptional networks (Bhadra and Ellington, 2014; Lucks et al., 2011; Nissim et al., 2014; Takahashi et al., 2015), and RNA-based diagnostics (Pardee et al., 2014).

For bacterial systems, small RNAs (sRNAs) have proven to be particularly well suited to engineering approaches that optimize and alter their function. Although sRNAs can act through a wide variety of mechanisms (Gottesman and Storz, 2011), a common mode of sRNA regulation relies on Watson–Crick base pairing between a sense target RNA, usually located upstream of the gene to be controlled, and a *trans*-acting antisense sRNA. By itself, the sense target RNA can fold into structures that block or allow gene expression—for example, by occluding a ribosome binding site, in the case of translation regulation, or forming an intrinsic terminator hairpin, in the case of transcription regulation. Interaction between the sense target RNA and antisense sRNA can then cause structural rearrangement, ultimately controlling the

expression of the gene. Years of research have uncovered design principles for these mechanisms, enabling engineers to create a wide array of sRNA regulators, including translational repressors (Mutalik et al., 2012; Na et al., 2013) translational activators (Green et al., 2014; Isaacs et al., 2004; Rodrigo et al., 2012), and transcriptional repressors (Lucks et al., 2011; Qi et al., 2012; Takahashi and Lucks, 2013).

Despite the versatility of engineered sRNA regulators, until recently there were no known natural or synthetic examples of sRNAs that could activate transcription (Chappell et al., 2013). To address this gap, we created small transcription activating RNAs (STARs) (Chappell et al., 2015) (Fig. 1A). In the STAR mechanism, the sense target region contains an intrinsic terminator hairpin, which terminates transcription in the OFF state, preventing read-through of the downstream gene. The STAR antisense contains a specific anti-terminator sequence that is designed to bind to the 5′ stem of the terminator in *trans* to prevent terminator formation and allow transcriptional read-through in the ON state. This mechanistic design strategy was applied to target a range of intrinsic terminators derived from natural sources, from the pbuE riboswitch to the pT181 plasmid copy control element, ultimately creating five different STARs that displayed a range of transcriptional activation from 3-fold to 94-fold (Chappell et al., 2015). In addition, orthogonality between these STARs and a preexisting library of RNA transcriptional repressors (Takahashi and Lucks, 2013) allowed the construction of two previously unattainable RNA-only logic gates (Chappell et al., 2015), demonstrating the potential of STARs for engineering sophisticated RNA genetic circuitry.

STARs thus represent a powerful expansion of the RNA engineering toolbox for precisely regulating gene expression and creating synthetic genetic networks. However, much work remains to be done to broadly optimize the fold activation of these new regulators. In particular, only two of the originally designed STARs showed levels of activation greater than 10-fold, thereby limiting the number of STARs useful in applications that require large differences between ON and OFF expression states. Here we remedy this by applying several sRNA engineering methods (Carrier and Keasling, 1999; Sakai et al., 2013) and gene expression optimization strategies to optimize the overall fold activation of weak STAR regulators. Specifically, we used a combination of promoter strength tuning and STAR antisense RNA stabilization and engineering strategies to improve fold activation from 5.4-fold ($\pm$ 2.2) to 13.4-fold ($\pm$ 3.8) for the pbuE STAR regulator. To confirm that our approach could be generalized, we then applied these strategies to the unrelated prgX STAR (derived from a conjugation control system terminator) to improve its fold activation from 2.1-fold ($\pm$ 0.4) to 14.6-fold ($\pm$ 3.7). This process also yielded multiple STAR variants for both systems with intermediate fold activation levels, showing that this strategy can be used to fine-tune STAR performance. Finally, although the optimization strategies required the addition of a significant amount of extra RNA sequence and structure, we demonstrated that orthogonality was preserved between the optimized STARs and a set of RNA transcriptional repressors. These optimization strategies open the door for creating a range of additional STARs for use in a broad array of biotechnologies.

Materials and Methods

Plasmid Construction and Cloning

STAR-mediated gene expression was tested with a two-plasmid system. Plasmids were constructed so that the sequence encoding each sense target RNA was placed downstream of a constitutive promoter and upstream of the coding sequence for the superfolder green fluorescent protein (SFGFP) reporter (Pédelacq et al., 2006), complete with its own ribosome binding site (Supplementary Fig. S1). Separate plasmids were constructed for STAR antisense

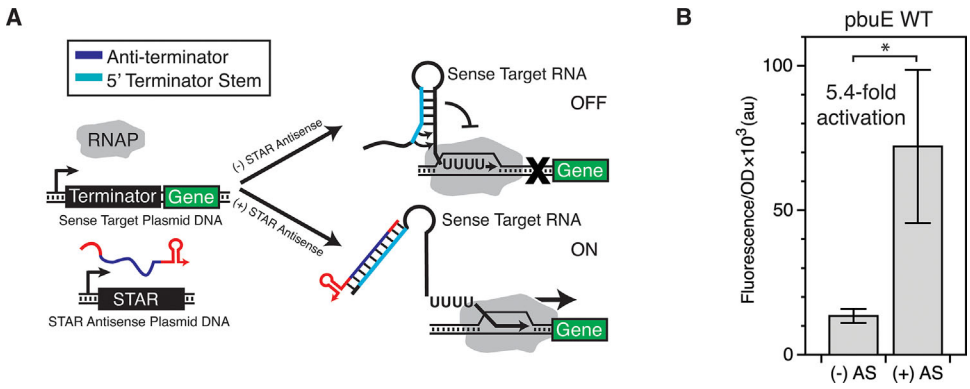

Figure 1. Design and function of a model Small Transcription Activating RNA (STAR). (**A**) Schematic of the mechanism following Chappell et al. (2015). In the absence of the STAR antisense, the nascent sense target RNA upstream of the reporter gene forms a terminator hairpin that stops transcription by RNA polymerase (RNAP) before the gene is transcribed (OFF). The STAR antisense is designed to contain an anti-terminator sequence complementary to the 5′ side of the terminator hairpin. When the STAR antisense is present, it binds to the terminator sequence, preventing formation of the terminator hairpin and allowing transcription of the downstream gene (ON). (**B**) In vivo characterization of the pbuE STAR regulator performed in this study using superfolder GFP (SFGFP) fluorescence to measure gene expression from a sense target plasmid with and without a STAR antisense (AS) plasmid. Normalized fluorescence was divided by OD_{600} (optical density at 600 nm) to give Fluorescence/OD, and fold activation was calculated as Fluorescence/OD ON divided by Fluorescence/OD OFF. Error bars represent sample standard deviation over three independent replicates with three colonies each ($n = 9$). The * symbol indicates a statistically significant ($P < 0.05$) increase in Fluorescence/OD in the case with STAR antisense as determined by a two-sided *T*-test.

expression, with the sequence encoding the STAR preceded by a constitutive promoter and followed by the t500 transcriptional terminator (Yarnell and Roberts, 1999) (Supplementary Fig. S1). For experiments in which the STAR antisense was absent, a control plasmid was constructed containing the constitutive promoter followed directly by a transcriptional terminator (rrnB terminator "TrrnB") (Supplementary Fig. S1).

All plasmids and sequences used in this study are enumerated in Supplementary Table S1. All sense target plasmids included the p15A origin and a gene for chloramphenicol resistance, while all STAR antisense plasmids contained the ColE1 origin and encoded a gene for carbenicillin resistance. All plasmids were either previously reported or constructed from previously reported plasmids (Chappell et al., 2015; Lucks et al., 2011; Takahashi and Lucks, 2013) using inverse polymerase chain reaction (iPCR) to make substitutions and/or insertions. The inserted sRNA scaffold and stability hairpin sequences were derived from previous work by Sakai et al. (2013) and Carrier et al. (1999), respectively. Sequence-verified stocks of the plasmids were used for all experiments.

Strains, Media, and In Vivo Bulk Fluorescence Experiments

All bulk fluorescence experiments were performed in *Escherichia coli* (*E. coli*) strain TG1 *(F'traD36 lacIq Delta(lacZ) M15 pro A+B+/ supE Delta(hsdM-mcrB) 5 (rk- mk- McrB-) thi Delta(lac-proAB))* with three independent replicates, except for the *hfq* knockout experiments (Fig. 3D), which were performed in *E. coli* strain BW25113 *(F⁻, DE(araD-araB) 567, lacZ4787(del)::rrnB-3, LAM⁻, rph-1, DE(rhaD-rhaB) 568, hsdR514)* and the BW25113 Δ*hfq* variant from the Keio collection (Baba et al., 2006). For each independent replicate, pairs of sense target plasmid and STAR antisense plasmid (or no-antisense control plasmid JBL002) were transformed into chemically competent *E. coli* TG1 cells, plated on Difco LB + Agar plates with 100 mg/mL carbenicillin and 34 mg/ml chloramphenicol, and incubated overnight at 37°C for approximately 17 h. For every experiment, the same procedure was repeated for the pair of empty autofluorescence control plasmids, JBL001 and JBL002, which did not express either STAR or sense target RNAs and were used to determine background cellular autofluorescence. After overnight incubation, the plates were removed from the incubator and kept at room temperature for approximately 7 h. Three separate colonies were picked for each condition/control, and each was used to inoculate 300 μL of LB media with 100 mg/mL carbenicillin and 34 mg/mL chloramphenicol in a 2 mL 96-well block (Costar 3960). In the case of the pbuE variants in Figure 4A, nine colonies were picked in order to guarantee enough passed the growth requirements described below. The block was covered with a breathable seal (Aeraseal BS-25) and incubated at 37°C while shaking at a speed of 1,000 rpm in a Labnet Vortemp 56 bench-top shaker for 18–19 h overnight. From this overnight culture 4 μL were taken and used to inoculate 196 μL of M9 minimal media (1 × M9 minimal salts, 1 mM thiamine hydrochloride, 0.4% glycerol, 0.2% casamino acids, 2 mM $MgSO_4$, 0.1 mM $CaCl_2$) containing 100 mg/mL carbenicillin and 34 mg/ml chloramphenicol. The cultures, alongside three wells of an M9 only control, were grown in a 2 mL 96-well block under the same conditions as the overnight culture, until the majority of the OD values exceeded 0.07, which took 5–7 h. Fifty microliters of this culture were diluted 1:1 with phosphate buffered saline (PBS) in a black-welled clear-bottomed 96-well plate (Costar 3231). The diluted cultures' optical density (OD) at 600 nm and fluorescence (485 nm excitation, 520 nm emission) were then measured with a Biotek Synergy H1 plate reader.

Data Analysis for Bulk Fluorescence Experiments

Each experiment included two sets of controls: three wells of a media blank (M9) and three wells inoculated from separate colonies of the autofluorescence control *E. coli* cells lacking SFGFP but harboring plasmids with the same backbones and resistances as all sense target and STAR antisense plasmids (transformed control JBL001 and JBL002). All fluorescence and OD values for each colony were initially corrected by subtracting the corresponding values from the average of the three media blanks. The ratio of fluorescence units over OD (Fluorescence/OD) was then calculated for each well and corrected for background fluorescence by subtracting the average Fluorescence/OD for the autofluorescence control cells without SFGFP. For each STAR-target pair, three independent colonies were characterized from three independent transformations (nine colonies total). Data were discarded for colonies that showed low growth ($OD < 0.07$), although this requirement was relaxed for the orthogonality grid in Figure 5 in order to account for the different growth rates of the tested variants. Averages and standard deviations (depicted by error bars) of Fluorescence/OD were calculated over the repeat experiments. Fold activation was calculated by dividing the average corrected Fluorescence/OD for a STAR-target pair (ON) by the average corrected Fluorescence/OD for the same sense target plasmid paired with the control no STAR antisense plasmid (JBL002) (OFF). Fold activation error was calculated using standard error propagation formulas based on the standard deviations of the average corrected Fluorescence/OD values. In calculating fold repression (Fig. 5), the negative reciprocal was taken to give the fold repression, that is, 0.20 became −5-fold repression (Chappell et al., 2015). Statistical significance calculations (two-sided *T*-tests) were performed on the individual colony Fluorescence/OD ON levels normalized by the average Fluorescence/OD OFF levels.

Results and Discussion

The pbuE STAR as a Case Study for Optimization of Fold Activation

As a starting point for exploring strategies to increase fold activation, we chose to focus on a STAR-target system (Chappell et al., 2015) derived from the intrinsic terminator of the pbuE riboswitch (Ceres et al., 2013b). As illustrated in Figure 1A, the pbuE STAR is designed to be fully complementary to the 5′ half of the pbuE intrinsic terminator present in the target RNA. Interaction of the STAR with its target RNA thus prevents the formation of the terminator hairpin, enabling transcription elongation into the downstream reporter gene, superfolder green fluorescent protein (SFGFP). To determine fold activation, gene expression was

characterized by measuring fluorescence normalized by optical density (Fluorescence/OD) for cultures of *E. coli* cells co-transformed with two plasmids: one plasmid encoding the pbuE sense target fused to the downstream SFGFP coding sequence and the other plasmid encoding either the STAR antisense (ON state) or an empty backbone control (OFF state) (absence of STAR antisense case). Activation was then calculated as a ratio of the ON/OFF Fluorescence/OD values (see Materials and Methods). Characterization of the pbuE STAR in this study reconfirmed its low fold activation, previously reported by Chappell et al. (2015), with an observed activation of 5.4-fold (± 2.2) in the presence of the STAR antisense compared to when only the target RNA was expressed (Fig. 1B). This result indicated that there was ample room for improvement in fold activation compared to the 94-fold (± 26) activation shown by the best STAR activator reported previously (Chappell et al., 2015). Furthermore, previous work on applying RNA sequence optimization strategies did not improve the low fold activation of the pbuE STAR system (Chappell et al., 2015), motivating us to pursue a suite of alternative strategies discussed below.

Improving Fold Activation of STARs by Manipulating STAR/Target Expression Ratios

To begin, we chose to investigate improving fold activation by increasing the relative concentration ratio of STAR antisense to its complementary sense target. A previously developed model of the STAR mechanism hypothesized that transcription activation is directly related to the rate of binding between STAR and target (Chappell et al., 2015). Therefore, increasing the expression level of the STAR antisense relative to its target should naturally increase the number of binding events, and thus increase the likelihood of any given target RNA being transcriptionally activated. To test this, we manipulated the STAR/target expression ratio in vivo in *E. coli* cells by altering the relative strengths of the constitutive promoters that drive the expression of the STAR antisense and sense target in our two-plasmid system (see Materials and Methods). Given that both the STAR and target RNAs were originally under the control of the same strong constitutive σ^{70} promoter, decreasing the strength of the sense target RNA promoter provided a straightforward way to titrate down the steady-state levels of sense target RNA by reducing the transcription rate. Following this strategy, we cloned a series of successively weaker constitutive promoters upstream of the pbuE sense target RNA and examined their effects on fold activation in vivo (Fig. 2). We chose promoters from the Anderson promoter library from the Registry of Standard Biological Parts (partsregistry.org), whose strengths have been well-characterized in previous work (Kelly et al., 2009) (Supplementary Table S2). The in vivo testing of these target promoter variants indicated that weakening the sense plasmid promoter strength did indeed result in greater fold activation, and we observed a clear correlation between decreased sense promoter strength and increased fold activation (Fig. 2B), with the majority of changes in fold activation being

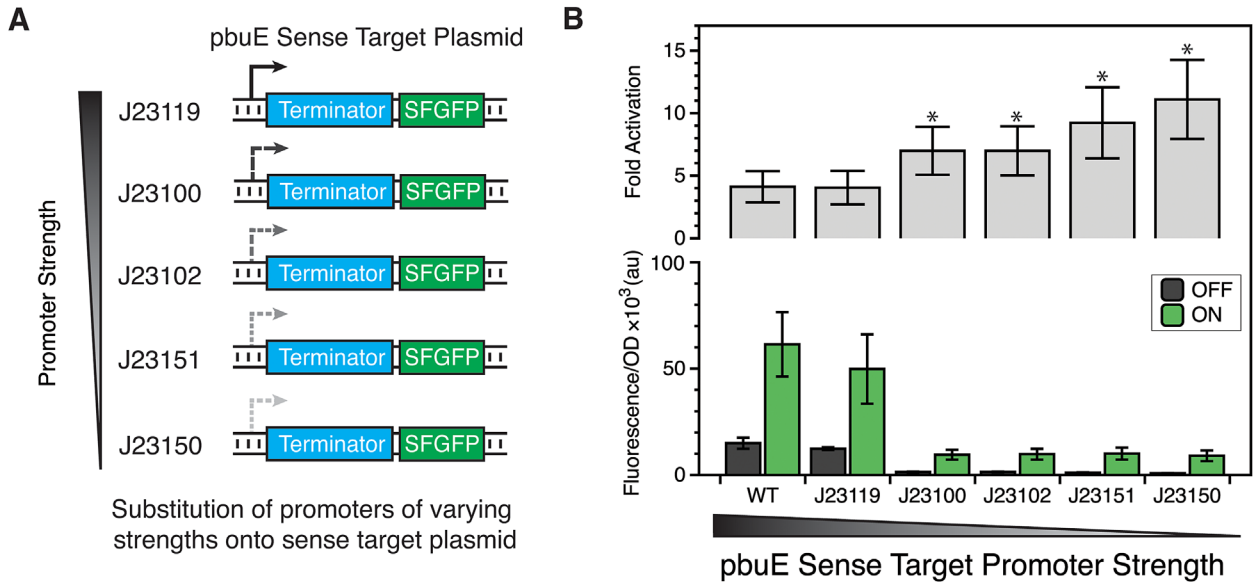

Figure 2. Optimization of the STAR/target expression ratio yields higher fold activation. (**A**) Schematic of the design strategy for improved activation. A number of weaker promoters were substituted for the strong wild-type (WT) promoter (J23119 SpeI) on the sense target plasmid in order to decrease the expression level of the sense RNA. In these experiments, the STAR was expressed from a high-copy plasmid using the strong J23119 SpeI promoter. This promoter series was designed to increase the relative expression ratio of STAR to target. (**B**) In vivo fluorescence characterization demonstrates an increase in fold activation when a weaker target promoter is used, with a fold activation of 11.1-fold (± 3.6) observed for the weakest J23150 promoter. Normalized fluorescence divided by optical density at 600 nm (Fluorescence/OD) is plotted on the lower axes, with the dark gray bars representing the OFF level (no-STAR control plasmid) and the green bars representing the ON level (STAR present). Fold activation (Fluorescence/OD ON divided by Fluorescence/OD OFF) is plotted on the upper axes as a series of light gray bars. Error bars represent sample standard deviation over three independent replicates with three colonies each ($n = 9$). The * symbol indicates statistically significant ($P < 0.05$) improvement in fold activation compared to the wild-type sense promoter configuration (J23119 SpeI) as determined by a two-sided *T*-test. Statistical significances of fold activation changes between different promoters are presented in Supplementary Table S3.

statistically significant (Supplementary Table S3). Although the overall ON level of fluorescence decreased as expected with a weaker promoter on the sense target reporter plasmid, we observed an even greater decrease in the OFF level that followed the same relative order as promoter strength (Kelly et al., 2009; Supplementary Table S2). This greater decrease in OFF level led to an overall increase in fold activation. When compared to the original promoter configuration, the weakest promoter tested, J23150, more than doubled the fold activation of the pbuE STAR regulator from 4.1-fold ($\pm$ 1.2) to 11.1-fold ($\pm$ 3.2). To further confirm that fold activation was directly related to the relative ratio of STAR to the sense target RNA, we characterized fold activation from the original pbuE sense target RNA as a function of decreased expression of the STAR using the same promoter series (Supplementary Fig. S2). As expected, lowering the STAR expression resulted in lower fold activation, confirming the importance of a high relative ratio of STAR antisense RNA to sense target RNA for high fold activation. Overall, our results demonstrate that we can increase the fold activation of STAR regulators through manipulating STAR/target expression ratios.

Improving Fold Activation of STARs by Engineering the STAR Antisense

Since manipulating RNA stability is a key point of control for RNA mechanisms (Chappell et al., 2013; Smolke and Keasling, 2002), we next sought to examine how altering the stability of the STAR antisense could be used as another strategy for improving fold activation. The steady-state level of STAR antisense molecules available for activation at any time is governed by the balance between two key rates: the rate of synthesis (transcription) and the rate of degradation. Since the STAR antisense was already expressed from a high-copy plasmid (ColE1 origin of replication) under the control of a strong promoter, reducing the degradation rate presented a more accessible way to increase the level of STAR antisense and thus fold activation. We sought to decrease the degradation rate of the STAR antisense by adding strong RNA hairpins to the 5′ end, following previous work using these hairpins to stabilize mRNAs (Carrier and Keasling, 1999) (Fig. 3A).

Our STAR stabilization strategy was based on the fact that secondary structures located at the 5′ end of bacterial mRNAs can confer stability (Carrier and Keasling, 1997; Emory et al., 1992) by blocking RNAse E-mediated degradation. In particular, this strategy has been shown to improve mRNA stability and lengthen mRNA half-lives (Carrier and Keasling, 1999). To investigate whether or not these stability hairpins added to STARs would improve fold activation, we added three previously published synthetic RNA stability hairpins (pHP14, pHP16, and pHP17) (Carrier and Keasling, 1999) to the 5′ end of the pbuE STAR. We then characterized the resulting fold activation of these modified STARs (Fig. 3B). Compared to the initial wild-type (WT) pbuE STAR, the variant with the added pHP16 5′ stability hairpin demonstrated modest, yet statistically significant, improvements in in vivo fold activation, going from 5.2-fold ($\pm$ 2.1) for the WT pbuE STAR to 7.7-fold ($\pm$ 2.2) with pHP16 (Fig. 3B). Interestingly, the level of increased activation did not directly correlate with the previously reported half-lives of these stability hairpins (Carrier and Keasling, 1999). While pHP14, pHP16, and pHP17 had been shown by Carrier and Keasling to confer successively longer half-lives (in numerical order), in the context of the pbuE STAR, only pHP16 appeared to confer a statistically significant increase in fold activation.

To test whether these hairpins conferred stability in the STAR context, we used RT-qPCR (reverse transcription quantitative polymerase chain reaction) to quantify the relative degradation of the pHP14, pHP16, and WT pbuE STAR variants at different time points after the addition of rifampicin to the media to halt transcription (see Supplementary Methods). We found that both pHP14 and pHP16 significantly reduced degradation of pbuE compared to the WT pbuE STAR (Supplementary Fig. S3) indicating that both hairpins do in fact stabilize the pbuE STAR. To understand why only modest levels of fold activation increase were observed with these hairpins, we used computational RNA structure modeling with RNAStructure (Reuter and Mathews, 2010) to predict the structures of the pbuE STAR variant with the added stability hairpins (Supplementary Fig. S4). This analysis showed that the stability hairpins could alter the predicted structure of the pbuE STAR RNAs. This folding could be enough to offset the benefits of increasing STAR stability, though in the case of pHP16 the benefits of stability outweighed the possible alteration of STAR structure.

As an alternate method of increasing fold-activation through engineering the STAR antisense, we tested adding sRNA-derived scaffolds to the 3′ end of the STAR, upstream of the transcriptional terminator. This strategy was based upon recent research (Na et al., 2013; Sakai et al., 2013; Sharma et al., 2012) showing that the addition of sRNA scaffolds to transcriptional and translational synthetic sRNA regulators can lead to improved function. Not only are the scaffolds theorized to stabilize the RNA through the addition of secondary structure, these particular sRNA-derived scaffolds are also designed to include binding sites for the RNA-binding chaperone protein Hfq. Among its many roles, Hfq is known to aid sRNA function by mediating sRNA interactions with target mRNAs for many trans-encoded sRNAs that regulate translation (Møller et al., 2002; Zhang et al., 2003). Hfq can also modulate sRNA stability by affecting ribonuclease accessibility or susceptibility to 3′ polyadenylation and subsequent degradation (Vogel and Luisi, 2011). To test the ability of sRNA scaffolds to increase fold activation for STAR regulators, we chose the MicF, Dsra1.3, and Spot42 scaffolds that were previously shown to lead to the greatest improvements in activation and repression levels in the RNA regulators tested (Sakai et al., 2013). We then fused each scaffold to the 3′ end of the pbuE STAR, directly before the transcriptional terminator (Fig. 3A). Functional testing in vivo showed variable results depending on the scaffold used. In particular, while the addition of the Spot42 scaffold to the pbuE STAR antisense slightly increased activation, both MicF and Dsra1.3 markedly decreased activation levels (Fig. 3C). Structural prediction with RNAStructure (Reuter and Mathews, 2010) indicated that a number of the most probable low-energy structures for the antisense fused with MicF or Dsra1.3 interfered with the native structure of both the STAR antisense and the sRNA scaffolds (Supplementary Fig. S5). Thus the observed decrease in activation in the case of the MicF and Dsra1.3 scaffolds could be

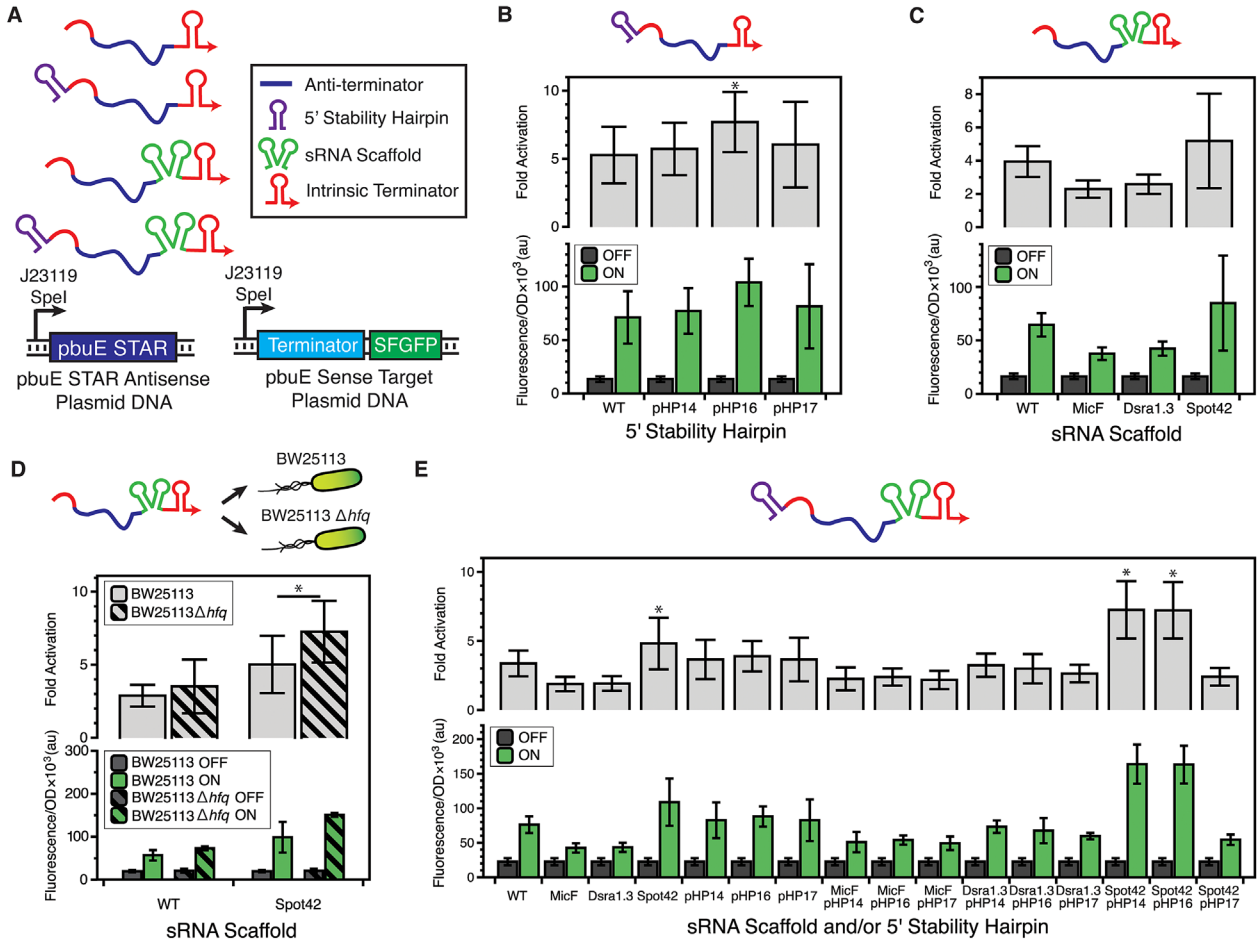

Figure 3. Improving fold activation by engineering the STAR antisense. (**A**) Schematic of the changes made to the pbuE STAR. Stability hairpins (purple) were added to the 5′ end of the pbuE STAR to block RNase E-mediated degradation (Carrier and Keasling, 1999). sRNA scaffolds (green) were added to the 3′ end to improve sRNA function, as previously demonstrated by Sakai et al. (2013). The J23119 SpeI promoter was used to express the pbuE STAR variant and sense target RNAs. Data are plotted as in Figure 2. (**B**) In vivo functional characterization of stability hairpin STAR variants indicates that the addition of the pHP16 5′ stability hairpin confers a modest increase in activation function to the pbuE STAR regulator. (**C**) In vivo functional characterization of sRNA scaffold pbuE STAR variants indicates that only the addition of the Spot42 sRNA scaffold results in a small increase in fold activation, though this is not statistically significant over the initial wild-type (WT) pbuE STAR. Addition of the MicF or Dsra1.3 sRNA scaffolds to the pbuE STAR was shown to decrease fold activation. (**D**) Testing of the Spot42 sRNA scaffold variant of the pbuE STAR in BW25113 and BW25113 Δ*hfq* strains demonstrates slightly *higher* activation levels in the absence of Hfq. (**E**) Combining both sRNA scaffolds and 5′ stability hairpins yields the highest fold activation for the combinations of Spot42/pHP14 and Spot42/pHP16. In parts (B), (C), and (E) the * symbol indicates a statistically significant ($P < 0.05$) increase in fold activation over WT as determined by a two-sided *T*-test. In part (D) * indicates a statistically significant ($P < 0.05$) difference in fold activation between the two strains tested as determined by a two-sided *T*-test.

the result of structural interference between the scaffold and the STAR.

While the Spot42 variant fold activation was statistically different from the other two scaffold variants, it was not statistically different from the WT pbuE STAR fold activation. Despite this, we did confirm that the Spot42 sRNA scaffold increased STAR stability compared to the WT pbuE STAR, though not as much as the pHP14 and pHP16 stability hairpins (Supplementary Fig. S3). Since it was the only functioning scaffold variant, we next sought to test the role of Hfq in the observed modest increase in STAR activation with the Spot42 scaffold. To test this, we repeated the in vivo functional characterization of the Spot42 fusions in both the Keio collection Δ*hfq* knockout strain and its parent *E. coli* K-12 BW25113 strain (Baba et al., 2006) (Fig. 3D). We found that the absence of Hfq had little to no effect on the wild-type pbuE STAR activation, as expected given that the wild-type does not contain an Hfq-recruiting scaffold sequence. Surprisingly, we found that the activation level of the pbuE STAR-Spot42 fusion significantly improved in the absence of Hfq, in contrast to previous observations of the reliance of sRNA scaffolds on Hfq for added stability (Sakai et al., 2013).

Next, we examined whether we could increase fold activation further by combining the stability hairpin and sRNA scaffold strategies together. To test this, we created all possible combinations of the pbuE STAR antisense containing both 5′ stability hairpins and 3′ sRNA scaffolds. In vivo characterization indicated that the combination of the Spot42 scaffold with either the pHP14 or pHP16 stability hairpin granted significantly improved activation over any

of the variants with only hairpin or scaffold (Fig. 3E). In particular, we observed 7.2-fold (± 2.1) activation for the variant with both Spot42 and pHP14 and 7.2-fold (± 2.0) activation for the variant with Spot42 and pHP16, both significantly better than the 4.8-fold (± 1.9) activation seen for Spot42 alone, though statistically indistinguishable from each other. The addition of both a 5′ stability hairpin and the Spot42 scaffold may alter the STAR structure so that it can fully benefit from the stabilization of the stability hairpin to increase overall fold activation.

Interestingly, these increases in fold activation are larger than the improvements in transcription repression seen when scaffolds were applied to the pT181 RNA-based transcriptional repressor (Sakai et al., 2013). However, Sakai et al. were able to successfully use these strategies to improve the fold activation of an RNA translational activator. These results could suggest a more general principle for antisense RNA engineering strategies being more effective for gene expression activation or could indicate these strategies are more effective when applied to relatively unstructured antisense RNAs.

Overall, our results showed that the incremental improvements in fold activation generated by the addition of 5′ stability hairpins and 3′ scaffolds alone can be combined to generate STARs with even higher fold activation. However, more work is needed to uncover the structural basis of non-functioning variants, as well as the synergistic effect among the functional variants in order to make this strategy more predictable.

A General Method for Increasing STAR Activation by Combining Expression Level Tuning and RNA Engineering Strategies

We subsequently investigated whether combining expression level tuning and RNA engineering strategies could be used to further optimize fold activation for the pbuE STAR. To do this, we combined the Spot42/pHP14 pbuE antisense variant together with the weakened promoter strength series on the sense target RNA. Combining the stabilized STARs with the weaker promoter sense target plasmids yielded another increase in activation level, reaching as high 13.4-fold (± 3.8) activation in the case of the Spot42 pHP14 antisense combined with the sense target plasmid containing the J23151 promoter (Fig. 4A). While the general trend was toward higher fold activation with weaker promoters, there was high error, and the trend was less uniform than seen previously, though the differences between the J23151 variant and all others were statistically significant. Nevertheless, the higher fold activation seen from combining the optimized pbuE STAR with weaker sense target promoters indicates that RNA engineering strategies can be combined with expression tuning to increase fold activation.

Having successfully optimized the pbuE transcriptional activator from its initial 5.3-fold (± 2.2) activation level to 13.4-fold (± 3.8) activation, we next sought to test the generality of this combined method for improving STAR fold activation. We started with a previously constructed STAR generated from the prgX conjugation

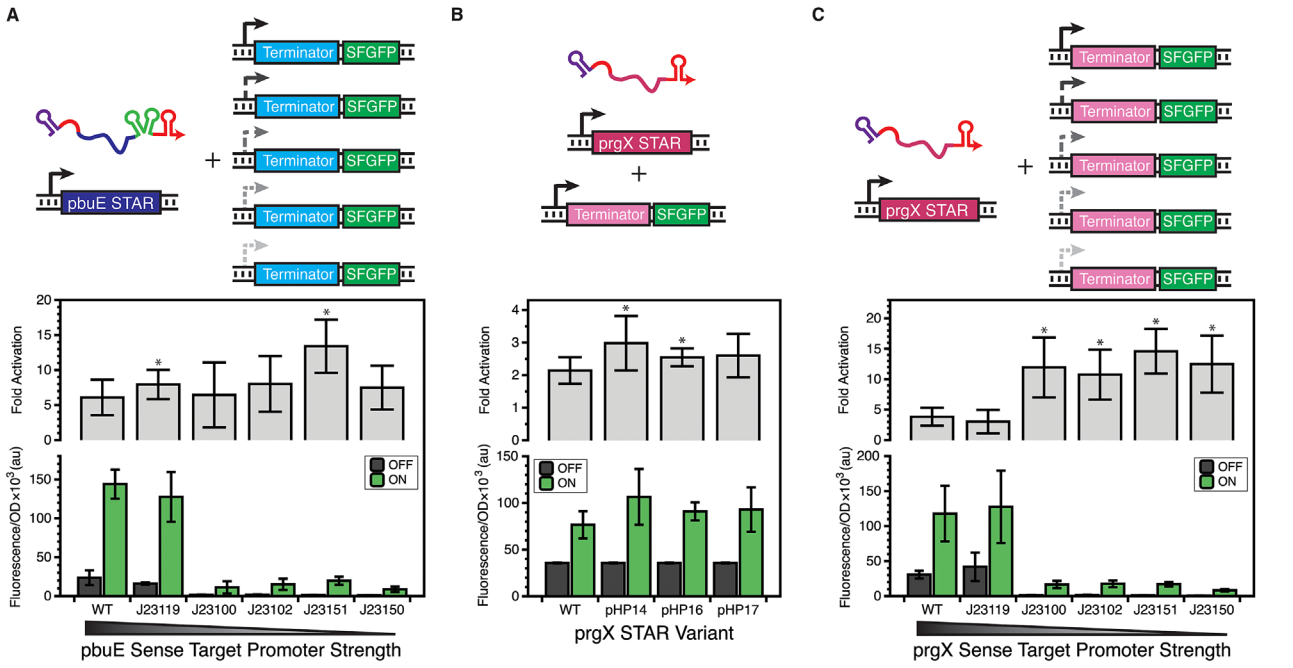

Figure 4. Combining expression level tuning and RNA engineering strategies improves STAR fold activation in multiple systems. Data are plotted as in Figure 2. (**A**) Combining the pbuE STAR antisense fused with the Spot42 scaffold and the pHP16 stability hairpin with weaker target sense promoters yields up to 13.4-fold (± 2.0) activation for the J23151 promoter pairing. (**B**) 5′ stability hairpins slightly improve fold activation for the prgX STAR regulator. (**C**) Combining the prgX STAR fused with the pHP14 stability hairpin with weaker strength target promoters yields another boost in fold activation, showing the broader applicability of these STAR optimization strategies. Wild-type (WT) indicates the initial pbuE STAR regulator in part (A) and the initial prgX STAR regulator in part (B) and (C), both of which use the strong J23119 SpeI promoter to drive both STAR and target RNAs. The * indicates a statistically significant ($P < 0.05$) increase in fold activation over WT, as determined by a two-sided *T*-test.

control system (Weaver, 2007) that only displayed a 2.1-fold (± 0.4) activation (Chappell et al., 2015) (Fig. 4B). In particular, we applied the same 5′ stability hairpins as used above and the Spot42 sRNA scaffold to the prgX STAR. In vivo testing revealed that while some of the hairpin additions modestly improved fold activation (Fig. 4B), the addition of the Spot42 scaffold did not (Supplementary Fig. S6). When combined with weaker sense target promoters, the best prgX STAR variant (pHP14) had an even greater increase in fold activation (Fig. 4C), providing further proof of the modularity of the strategies for modifying sense promoter and STAR antisense stability. Overall, the best prgX variant displayed 14.6-fold (± 3.7) activation, a vast improvement from the original 2.1-fold (± 0.5) activation and a validation that the optimization strategies work on an additional, unrelated STAR system.

Testing the Orthogonality of Optimized STARs to Each Other and to RNA Transcriptional Repressors

We next sought to test whether the best variants of our two newly optimized STARs were orthogonal to the previously reported ribA STAR (Chappell et al., 2015) and three previously developed transcriptional repressors (Lucks et al., 2011; Takahashi and Lucks, 2013). If two regulators are orthogonal, then the antisense of one should not regulate the sense target RNA of the other (and vice versa), allowing them to be used together in a complex regulatory system without cross-talk. Such orthogonality is non-trivial, especially given that the inclusion of additional RNA sequence within the optimized STARs increases the potential for off–target interactions, as does increasing the concentration ratios of STARs to their targets. Moreover, orthogonality of these component parts is key for their use in the higher-order logic gates and circuits that STARs and transcriptional repressors have been used to construct (Chappell et al., 2015; Lucks et al., 2011; Takahashi and Lucks, 2013). For example, the ability to build circuits using orthogonal elements allows synthetic biologists to program systems with complex functionalities like ligand-sensitive NOR gates (Qi et al., 2012) and RNA cascades that control the timing of gene expression (Takahashi et al., 2015), a vital capability for biotechnology applications.

To perform the orthogonality test, we challenged each optimized STAR antisense variant against the sense targets from the pbuE and prgX systems (using the J23151 promoter), along with the sense target from the previously reported ribA STAR (Chappell et al., 2013). We also checked for orthogonality to sense target regions from three RNA transcriptional repressors: pT181.H1 from Lucks et al. (2011); Fusion 4, and Fusion 6 from Takahashi and Lucks (2013). As a further test, we challenged each RNA transcriptional repressor antisense variant against the same set of sense targets. This resulted in a 6 × 6 matrix of conditions demonstrating the observed orthogonality of these regulators to one another (Fig. 5, Supplementary Fig. S7). Both of the newly optimized STARs showed reasonable orthogonality to the other regulators. We did observe that the only off-target activation was between the pbuE STAR

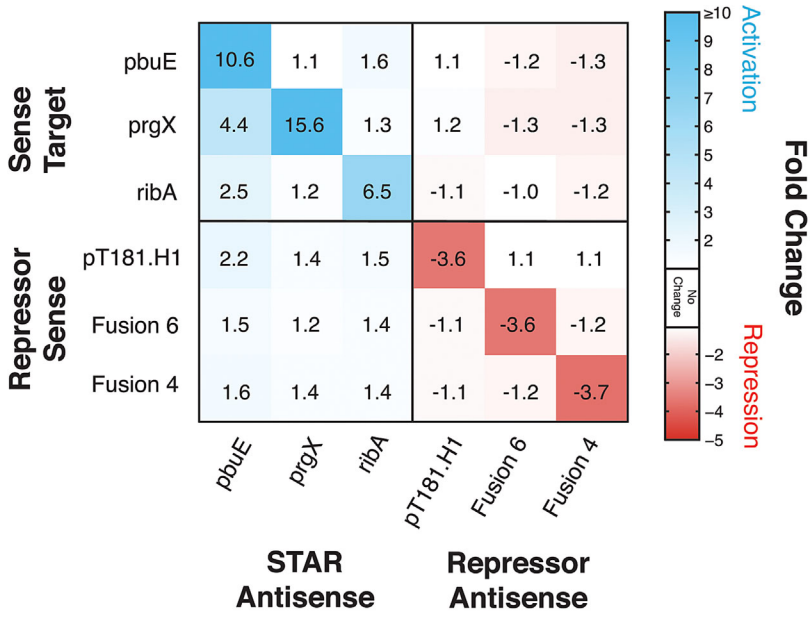

Figure 5. Testing the orthogonality of improved STAR regulators with each other and with RNA transcriptional repressors. Characterization of a 6 × 6 orthogonality matrix consisting of the newly optimized pbuE and prgX STAR regulators, the previously reported ribA STAR regulator (Chapell et al., 2015), the pT181.H1 repressor (Lucks et al., 2011) and Fusion 4 and Fusion 6 transcriptional repressors reported by Takahashi and Lucks (2013). Each matrix square represents the fold change of gene expression for the indicated combination of STAR or repressor plasmid and target plasmid, compared to the condition with target plasmid and an empty no-antisense control plasmid. Fluorescence characterization (measured in units of Fluorescence/OD, fluorescence divided by optical density at 600 nm) was used to calculate average fold change, which is represented by a color scale in which ≥10-fold is the darkest blue (activation), 1-fold is white (no activation or repression) and -5-fold is red (repression). Fluorescence/OD plots for each individual combination are shown in Supplementary Fig. S7. Data represents mean values of $n = 9$ biological replicates.

antisense and the prgX, ribA and pT181.H1 sense targets, though this effect was well below the activation seen with its cognate target, and was associated with high experimental variability (Supplementary Fig. S7). More work is needed to understand the nature of the transient interactions that may occur between STARs and their potential targets during the dynamic process of transcription to understand this effect.

These results confirm that these STAR optimization strategies largely do not affect the orthogonality of STARs between themselves and RNA transcriptional repressors. Not only will the addition of new orthogonal STARs allow for more complex RNA circuitry, the optimization strategies used to improve STAR activation will allow for the future development of more highly functional RNA transcriptional activators.

Conclusions

In this work, we tested several RNA engineering strategies for optimizing the fold activation of small transcription activating RNAs. In particular, we focused on strategies designed to stabilize and improve the STAR antisense design and alter the concentration ratio between the STAR and its target. Using the pbuE STAR as a test case, we showed that the addition of 5′ stability hairpins and sRNA scaffolds to the STAR antisense and the ability to adjust the ratio of STAR antisense to target sense via promoter strength tuning gave convenient and sometimes modular ways to alter the transcription activation levels of two distinct STAR systems. Specifically, we found that these strategies as applied to the pbuE STAR system increased the fold activation from 5.3-fold ($\pm$ 2.2) to 13.4-fold ($\pm$ 3.8). Moreover, we showed that these strategies were general and, when applied to the unrelated prgX STAR regulator, yielded an increase in transcription activation from 2.1-fold ($\pm$ 0.4) to 14.6-fold ($\pm$ 3.7). Furthermore, we showed that these changes largely preserved the orthogonality of the optimized STARs to each other and to a panel of RNA transcriptional repressors that have been used to construct higher-order RNA transcriptional circuits (Chappell et al., 2015; Lucks et al., 2011).

These results are significant for several reasons. First, these optimizations have expanded the repertoire of STARs—the starting point fold activations for the pbuE and prgX STAR regulators prohibited their use for higher order circuit construction, a problem remedied by our optimizations. Second, the optimization strategies used on the pbuE and prgX systems should be applicable to many other STARs, paving the way for even larger libraries of RNA regulators. Finally, the demonstrated orthogonality between the newly optimized activators and previously reported regulators, in addition to representing a non-trivial achievement, makes them highly useful for future circuit-building.

It should be noted that the majority of the improvement in STAR fold activation was achieved through decreasing the OFF level. If a high ON level were required for a particular application, other strategies could be used to increase ON levels while maintaining low OFF levels. For instance, if high protein expression were desired, modular strategies aimed at tuning translation through altering ribosome binding site strength and accessibility could be used as an alternate way of manipulating target gene expression levels (Salis et al., 2009).

In addition to optimizing STAR fold activation, the tested strategies have led to a series of STARs with varying ON, OFF, and fold activation levels. These strategies have thus created a panel of variants that can be used for fine-tuning of transcription activation. The importance of fine-tuning individual regulators to enable the correct performance of a larger circuit has been demonstrated in numerous examples of synthetic circuits (Ellis et al., 2009; Elowitz and Leibler, 2000; Wang et al., 2009), making the suite of functional STAR variants a useful library to draw from for future circuit design. Strategies like these are becoming more important as synthetic biology looks to implement increasingly sophisticated genetic circuitry, requiring the ability to carefully tune the biological circuit components.

In summary, we have successfully expanded our capabilities for genetic regulation and made highly useful additions to the synthetic biology toolkit through systematic optimizations of a set of small transcription activating RNAs. These newly-improved STAR regulators will allow for the construction of complex cellular circuitry, and the optimization strategies will be highly useful for creating a generation of additional STARs for use in a broad range of biotechnologies.

We thank Professor Matthew DeLisa (Cornell Chemical and Biomolecular Engineering) for providing the BW25113 and BW25113 *Δhfq* strains. This material is based upon work supported by the National Science Foundation Graduate Research Fellowship Program [DGE-1144153 to S.M.], the Cornell University College of Engineering 'Engineering Learning Initiatives' Undergraduate Research Grant Program [to S.S. and R.C.], Defense Advanced Research Projects Agency Young Faculty Award (DARPA YFA) [N66001-12-1-4254 to J.B.L.], an Office of Naval Research Young Investigators Program Award (ONR YIP) [N00014-13-1-0531 to J. B. L.], and an NSF CAREER Award [1452441 to J. B. L.] J.B.L. is an Alfred P. Sloan Research Fellow.

References

Baba T, Ara T, Hasegawa M, Takai Y, Okumura Y, Baba M, Datsenko KA, Tomita M, Wanner BL, Mori H. 2006. Construction of *Escherichia coli* K-12 in-frame, single-gene knockout mutants: The Keio collection. Mol Syst Biol 2:1–11.

Bhadra S, Ellington AD. 2014. Design and application of cotranscriptional non-enzymatic RNA circuits and signal transducers. Nucleic Acids Res 42:e58.

Brantl S, Wagner EG. 2000. Antisense RNA-mediated transcriptional attenuation: An in vitro study of plasmid pT181. Mol Microbiol 35:1469–1482.

Carrier TA, Keasling JD. 1997. Controlling messenger RNA stability in bacteria: Strategies for engineering gene expression. Biotechnol Prog 13:699–708.

Carrier TA, Keasling JD. 1999. Library of synthetic 5' secondary structures to manipulate mRNA stability in *Escherichia coli*. Biotechnol Prog 15:58–64.

Cech TR, Steitz JA. 2014. The noncoding RNA revolution — trashing old rules to forge new ones. Cell 157:77–94.

Ceres P, Garst AD, Marcano-Velázquez JG, Batey RT. 2013a. Modularity of select riboswitch expression platforms enables facile engineering of novel genetic regulatory devices. ACS Synth Biol 2:463–72.

Ceres P, Trausch JJ, Batey RT. 2013b. Engineering modular "ON" RNA switches using biological components. Nucleic Acids Res 41:10449–10461.

Chappell J, Takahashi MK, Lucks JB. 2015. Creating small transcription activating RNAs. Nat Chem Biol 11:214–220.

Chappell J, Takahashi MK, Meyer S, Loughrey D, Watters KE, Lucks JB. 2013. The centrality of RNA for engineering gene expression. Biotechnol J 8:1379–1395.

Collins JA, Irnov I, Baker S, Winkler WC. 2007. Mechanism of mRNA destabilization by the *glmS* ribozyme. Genes Dev 21:3356–3368.

DebRoy S, Gebbie M, Ramesh A, Goodson JR, Cruz MR, van Hoof A, Winkler WC, Garsin DA. 2014. A riboswitch-containing sRNA controls gene expression by sequestration of a response regulator. Science 345:937–940.

Ellis T, Wang X, Collins JJ. 2009. Diversity-based, model-guided construction of synthetic gene networks with predicted functions. Nat Biotechnol 27:465–71.
Elowitz MB, Leibler S. 2000. A synthetic oscillatory network of transcriptional regulators. Nature 403:335–338.
Emory SA, Bouvet P, Belasco JG. 1992. A 5'-terminal stem-loop structure can stabilize mRNA in *Escherichia coli*. Genes Dev 6:135–148.
Filipowicz W, Bhattacharyya SN, Sonenberg N. 2008. Mechanisms of post-transcriptional regulation by microRNAs: Are the answers in sight? Nat Rev Genet 9:102–114.
Gottesman S, Storz G. 2011. Bacterial small RNA regulators: Versatile roles and rapidly evolving variations. Cold Spring Harb Perspect Biol 3.
Green AA, Silver PA, Collins JJ, Yin P. 2014. Toehold switches: De-Novo-designed regulators of gene expression. Cell 159:1–15.
Isaacs FJ, Dwyer DJ, Ding C, Pervouchine DD, Cantor CR, Collins JJ. 2004. Engineered riboregulators enable post-transcriptional control of gene expression. Nat Biotechnol 22:841–847.
Kelly JR, Rubin AJ, Davis JH, Ajo-Franklin CM, Cumbers J, Czar MJ, de Mora K, Glieberman AL, Monie DD, Endy D. 2009. Measuring the activity of BioBrick promoters using an in vivo reference standard. J Biol Eng 3:4.
Kennedy AB, Vowles JV, d'Espaux L, Smolke CD. 2014. Protein-responsive ribozyme switches in eukaryotic cells. Nucleic Acids Res 42:12306–12321.
Lucks JB, Qi L, Mutalik VK, Wang D, Arkin AP. 2011. Versatile RNA-sensing transcriptional regulators for engineering genetic networks. Proc Natl Acad Sci 108:8617–8622.
Lynch SA, Desai SK, Sajja HK, Gallivan JP. 2007. A high-throughput screen for synthetic riboswitches reveals mechanistic insights into their function. Chem Biol 14:173–184.
Møller T, Franch T, Højrup P, Keene DR, Bächinger HP, Brennan RG, Valentin-Hansen P. 2002. Hfq: A bacterial Sm-like protein that mediates RNA-RNA interaction. Mol Cell 9:23–30.
Mutalik VK, Qi L, Guimaraes JC, Lucks JB, Arkin AP. 2012. Rationally designed families of orthogonal RNA regulators of translation. Nat Chem Biol 8:447–454.
Na D, Yoo SM, Chung H, Park H, Park JH, Lee SY. 2013. Metabolic engineering of *Escherichia coli* using synthetic small regulatory RNAs. Nat Biotechnol 31:170–174.
Nissim L, Perli SD, Fridkin A, Perez-Pinera P, Lu TK. 2014. Multiplexed and programmable regulation of gene networks with an integrated RNA and CRISPR/Cas toolkit in human cells. Mol Cell 54:698–710.
Nou X, Kadner RJ. 2000. Adenosylcobalamin inhibits ribosome binding to *btuB* RNA. Proc Natl Acad Sci 97:7190–7195.
Pardee K, Green AA, Ferrante T, Cameron DE, DaleyKeyser A, Yin P, Collins JJ. 2014. Paper-based synthetic gene networks. Cell 159:940–954.
Pédelacq J-D., Cabantous S, Tran T, Terwilliger TC, Waldo GS. 2006. Engineering and characterization of a superfolder green fluorescent protein. Nat Biotechnol 24:79–88.
Qi LS, Lucks JB, Liu CC, Mutalik VK, Arkin AP. 2012. Engineering naturally occurring trans-acting non-coding RNAs to sense molecular signals. Nucleic Acids Res 40:5775–5786.
Reuter JS, Mathews DH. 2010. RNAstructure: Software for RNA secondary structure prediction and analysis. BMC Bioinformatics 11:129.
Rodrigo G, Landrain TE, Jaramillo A. 2012. De novo automated design of small RNA circuits for engineering synthetic riboregulation in living cells. Proc Natl Acad Sci 109:15271–15276.
Sakai Y, Abe K, Nakashima S, Yoshida W, Ferri S, Sode K, Ikebukuro K. 2013. Improving the gene-regulation ability of small RNAs by scaffold engineering in *Escherichia coli*. ACS Synth Biol 3:152–162.
Salis HM, Mirsky EA, Voigt CA. 2009. Automated design of synthetic ribosome binding sites to control protein expression. Nat Biotechnol 27:946–950.
Sharma V, Yamamura A, Yokobayashi Y. 2012. Engineering artificial small RNAs for conditional gene silencing in *Escherichia coli*. ACS Synth Biol 1:6–13.
Smolke CD, Keasling JD. 2002. Effect of copy number and mRNA processing and stabilization on transcript and protein levels from an engineered dual-gene operon. Biotechnol Bioeng 78:412–424.
Storz G, Vogel J, Wassarman KM. 2011. Regulation by small RNAs in bacteria: Expanding frontiers. Mol Cell 43:880–891.
Takahashi MK, Chappell J, Hayes CA, Sun ZZ, Kim J, Singhal V, Spring KJ, Al-Khabouri S, Fall CP, Noireaux V, Murray RM, Lucks JB. 2015. Rapidly characterizing the fast dynamics of RNA genetic circuitry with cell-free transcription-translation (TX-TL) systems. ACS Synth Biol 4:503–515.
Takahashi MK, Lucks JB. 2013. A modular strategy for engineering orthogonal chimeric RNA transcription regulators. Nucleic Acids Res 41:7577–7588.
Vogel J, Luisi BF. 2011. Hfq and its constellation of RNA. Nat Rev Microbiol 9:578–589.
Wachsmuth M, Findeiß S, Weissheimer N, Stadler PF, Mörl M. 2013. *De novo* design of a synthetic riboswitch that regulates transcription termination. Nucleic Acids Res 41:2541–2551.
Wang HH, Isaacs FJ, Carr PA, Sun ZZ, Xu G, Forest CR, Church GM. 2009. Programming cells by multiplex genome engineering and accelerated evolution. Nature 460:894–898.
Weaver KE. 2007. Emerging plasmid-encoded antisense RNA regulated systems. Curr Opin Microbiol 10:110–116.
Winkler W, Nahvi A, Breaker RR. 2002. Thiamine derivatives bind messenger RNAs directly to regulate bacterial gene expression. Nature 419:952–956.
Xie Z, Wroblewska L, Prochazka L, Weiss R, Benenson Y. 2011. Multi-input RNAi-based logic circuit. Science 333:1307–1311.
Yarnell WS, Roberts JW. 1999. Mechanism of intrinsic transcription termination and antitermination. Science 284:611–615.
Zhang A, Wassarman KM, Rosenow C, Tjaden BC, Storz G, Gottesman S. 2003. Global analysis of small RNA and mRNA targets of Hfq. Mol Microbiol 50:1111–1124.

Supporting Information

Additional supporting information may be found in the online version of this article at the publisher's web-site.